Preliminary Study on a Simplified Two-Phase-Flow Model for the Dynamics of Passive Emergency Core Cooling System Valves

Jeong-won Han [a], Young Seok Bang [a], Youngjae Park [a*]
[a]*FNC Technology Co., Ltd., 13 Heungdeok 1-ro, Giheung-gu Yongin-si, Gyeonggi-do, Republic of Korea*
[*]*Corresponding author: ypark1227@fnctech.com*

Keywords : i-SMR, PECCS valves, Dynamic behavior analysis, Two-phase, MATLAB

1. Introduction

The valves of PECCS (Passive Emergency Core Cooling System) of i-SMR (Innovative Small Modular Reactor) are driven by the pressure difference between the reactor pressure vessel and the containment vessel [1]. In the arrangement considered here the differential pressure holds the valve closed and keeps the spring deflected, and the spring drives the disk open as the vessel depressurizes. The valve therefore opens when the differential pressure falls to the value at which the two forces balance. With no electrical actuation involved, the time at which that balance is reached is part of the safety function to be evaluated. A lumped-parameter, multi-control-volume program was developed for this purpose on a single-phase basis [1] and was later extended to two-phase flow with the disk held fixed [2].

The discharged coolant is close to saturation and may flash, that is, boil as the pressure falls. Flashing changes the depressurization rate in two ways. The choked mass flow rate of a two-phase mixture is far below that of the subcooled liquid it replaces, so the vessel empties more slowly. The vapour generated inside the vessel also resists further pressure reduction. Both act on the pressure that drives the valve, so the phase change enters the force balance itself. This paper reports the interim status of a development in which the disk equation of motion is coupled to the two-phase chamber model. A similar coupling of a disk equation of motion to a vessel pressure equation has been used to estimate the opening time of a direct spring operated relief valve in multiphase flow [3]. That treatment excludes phase change, and its authors state that it is not applicable to flashing flow.

2. Modeling

2.1 Coupled Valve-Chamber Model

Figure 1 shows the arrangement, which is an idealized representation rather than a specific design. The disk is pressed onto its seat by the differential pressure acting on the pressure area A_p, and the deflected spring acts in the opening direction, so the valve stays closed while the differential pressure exceeds $\Delta p_{open} = s\, z_0 / A_p$. The coupling runs both ways: the chamber pressures set the force on the disk, and the disk position sets the throat area and the chamber volumes.

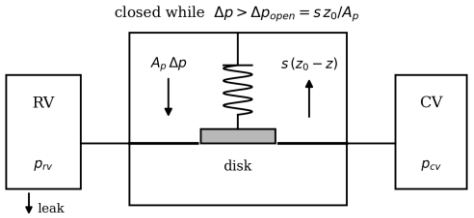


Fig. 1. Idealized valve arrangement: the differential pressure on A_p holds the disk closed and the deflected spring drives it open.

The valve interior is represented by control volumes connected by flow paths, so that the pressure difference between chambers, which is what moves the disk, is resolved rather than assumed. Each interior control volume is described by its mass, total enthalpy and pressure, and the chambers are adiabatic. The pressure rate is closed from the equation of state $\rho = \rho(P, h)$ of the IAPWS-IF97 industrial formulation, so that the two-phase compressibility, including the phase-change contribution, is carried consistently [2]:

$$\frac{dm_i}{dt} = \sum_{in} \dot{m} - \sum_{out} \dot{m} \qquad (1)$$

Here i denotes the control volume, ṁ the mass flow rate, h the specific enthalpy and V the volume. The term dV_i/dt vanishes when the disk is fixed and is retained here. The disk is treated as a single degree of freedom oscillator:

$$\frac{d(m_i h_i)}{dt} = \sum_{in} \dot{m}\; h_{in} - \sum_{out} \dot{m}\; h_i + V_i \frac{dP_i}{dt} \qquad (2)$$

where z is the lift, m the moving mass, s the spring stiffness, k the viscous damping coefficient and z_0 the spring deflection at the closed position. The lift sets the throat area, taken as the smaller of the bore area and the curtain area, which is the cylindrical gap the disk uncovers as it rises.

The damping is set to a lower bound, following the practice of the relief-valve literature, in which artificial damping is not permitted in a calculation of opening time [3]. The steady flow force is omitted. Each vessel is a single homogeneous control volume, so phase separation inside a vessel is not represented; of these

three simplifications the last is probably the strongest for the slowly opening cases of Section 5.

2.2 Critical-Flow Model

The discharge is obtained from the homogeneous equilibrium relation in which the compressibility of the mixture is carried by a single dimensionless parameter ω [4], in the form given for pressure safety valves by Boccardi et al. [5]. It was adopted because it is available in closed form, so it can be evaluated inside the right-hand side of a stiff ordinary differential equation. It also covers choked and unchoked flow and saturated, two-phase and subcooled inlets within one framework [5], which the present cases require because the inlet state changes during a single transient. Below a critical pressure ratio the flow chokes, so that lowering the downstream pressure no longer increases the flow rate. The critical pressure ratio and the dimensionless mass flux are

$$\frac{dP_i}{dt} = \frac{(\dot{m}_{in}-\dot{m}_{out})-\left(\frac{\partial\rho}{\partial h}\right)_P \frac{\dot{m}_{in}(h_{in}-h_i)}{\rho_i} - \rho_i \frac{dV_i}{dt}}{V_i\left[\left(\frac{\partial\rho}{\partial P}\right)_h + \frac{1}{\rho_i}\left(\frac{\partial\rho}{\partial h}\right)_P\right]} \tag{3}$$

$$m\ddot{z} + k\dot{z} = s\,(z_0 - z) - A_p\,\Delta p \tag{4}$$

where η is the ratio of throat pressure to upstream stagnation pressure. The correlation is stated to apply away from the thermodynamic critical point, at a reduced temperature below 0.9 or a reduced pressure below 0.5, where both are normalized by their values at that point [5]. For an initially subcooled inlet the parameter is anchored on the saturation pressure of the inlet temperature instead, and the treatment then divides into a low and a high subcooling region [5]. Which of the two forms the present implementation follows has not been confirmed. Measurements on a real safety valve in steam and water report that a homogeneous equilibrium description underestimates the mass flow rate there, so that a two-phase discharge coefficient larger than the vapour coefficient is required [5]. Whether that direction holds for the present configuration is not known, so no conservative direction is assumed. A unit discharge coefficient is used here, which amounts to assuming that the ideal-nozzle model is exact; for two-phase flow no tabulation of valve discharge coefficients exists and the few reported values are sparse [5].

3. Simulation Conditions

The analysis object is the closed system of Fig. 1: an upstream vessel, the valve and a downstream vessel. Both vessel pressures are calculated, so the downstream pressure rises during the discharge and the downstream condition quoted below Table I is an initial condition rather than a fixed boundary. A leak is imposed on the upstream vessel at 1 s, so that the initial state is confirmed first, and all times are measured from the start of the calculation. The reported opening time is the instant of first lift. Two configurations are used. They differ in the initial upstream pressure and in Δp_{open}, and within each only the upstream fluid state is varied; the inlet temperatures straddle the saturation temperature corresponding to Δp_{open}, given in the table headers. The r column of Table I is the saturation pressure of the upstream fluid divided by Δp_{open}, and Section 5.2 explains why that ratio orders the cases. Configuration B supplies the two cases discussed in Section 5.1, and configuration A tests whether the same boundary in r holds at a markedly different absolute pressure. The conditions are a parametric test bed and are not intended to represent a specific accident scenario.

Table I: Cases discussed in Section 5

Case	r [-]	t_{open} [s]
Configuration A: 4.5 MPa initial, Δp_{open} approx. 2.19 MPa, $T_{sat}(\Delta p_{open})$ = 217.0 °C		
subcooled 230 °C	1.28	987
Configuration B: 15 MPa initial, Δp_{open} approx. 1.5 MPa, $T_{sat}(\Delta p_{open})$ = 198.3 °C		
subcooled 185 °C	0.75	9.9
subcooled 300 °C	5.73	2277
saturated, x = 0	10.0	1625

x is the inlet quality. The downstream initial condition is 0.01 MPa and 150 °C in both configurations.

4. Verification

Verification is reported in three categories: code verification against known answers, solution verification against numerical error, and the uncertainty from the choice of closure. The third is checked against a slip model and a non-equilibrium model, because comparing one homogeneous equilibrium formulation with another would not be an independent check. Validation against an experiment or a system code has not been performed. Table II lists the status reached so far.

Table II: Status of the verification

Item	Status
Critical pressure ratio at ω = 1 against exp(−1/2)	exact
Mass flux at that ratio against its closed form	machine precision
Zero flow through a path sealed on both sides	exact
Mass and energy residual against the integration error	[TBD]
Sensitivity to the tolerance and the maximum step	[TBD]
Cross-comparison against a slip and a non-equilibrium model	in progress
Comparison with experiment or a system code	not performed

The reduced pressure and temperature were also checked against the limits of the correlation. Configuration A lies inside throughout. In configuration B the subcooled cases satisfy the temperature limit, whereas the saturated cases start outside both and re-

enter as the system depressurizes, so for those the early transient is an extrapolation.

5. Results and Discussion

5.1 Effect of Upstream Fluid State

All values in this section are calculated with the present model. Two cases of configuration B are compared; they share every input except the upstream fluid temperature. Figures 2 and 3 show the pressures, the disk lift and the mass flow rates for each. In every frame the broken vertical line marks the instant at which the calculated upstream pressure reaches the saturation pressure of the upstream temperature, which is where flashing begins. The horizontal line in the pressure frame is that saturation pressure.

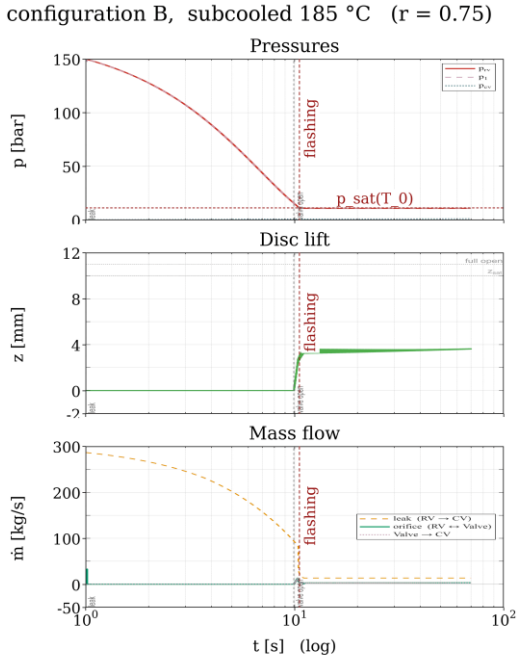


Fig. 2. Subcooled 185 °C case of configuration B. The disk lifts at 9.9 s, about 0.6 s before the upstream pressure reaches $p_{sat}(T_0)$ = 1.12 MPa.

In the 185 °C case of Fig. 2 the upstream fluid stays liquid and nearly incompressible while the leak drains it, the pressure falls steeply, and the disk first lifts at 9.9 s. The saturation pressure of 185 °C is only about 1.12 MPa, well below the opening threshold, so the falling pressure reaches the opening value first and flashing begins about 0.6 s later, at about 10.5 s. That margin is small, so this case sits close to the state at which the two events change order. The lift trace also shows that the disk did not reach its fully open position, which is taken up in Section 5.3.

In the 300 °C case of Fig. 3 the saturation pressure is about 8.59 MPa. The same rapid depressurization reaches it at about 10.5 s, within a fraction of a second of the onset in the other case, but this time before the opening value rather than after it. The upstream pressure then holds at a nearly constant level over more than two decades of time. The leak flow falls at that instant to about a quarter of its initial value, because the choked mass flow rate drops once the discharged fluid is two-phase. The disk first lifts only at 2277 s, by which time the downstream pressure has risen to about half the upstream value.

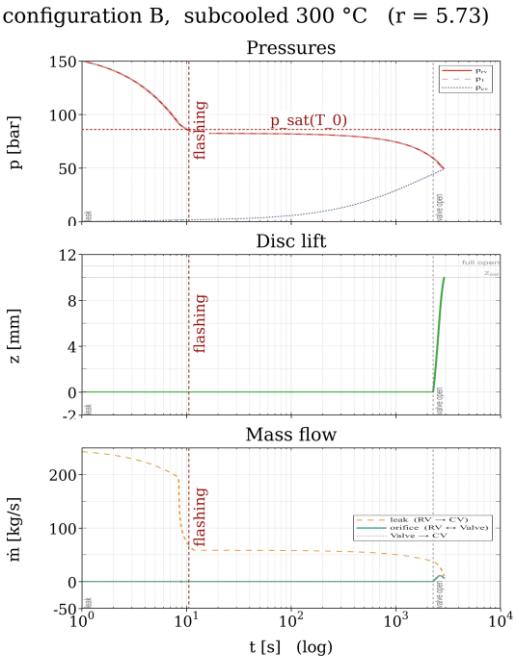


Fig. 3. Subcooled 300 °C case of configuration B. Flashing begins at about 10.5 s, before the disk first lifts at 2277 s.

The two cases differ by a factor of about 230 in opening time although flashing begins at essentially the same instant in both. What distinguishes them is not when flashing begins but whether it begins before or after the valve starts to open. In the 185 °C case the disk lifts while the fluid is still single phase, so a single-phase calculation would be expected to reproduce that opening time, whereas the delayed cases arise from the pressure stall that follows flashing. That comparison has not been run.

5.2 Flashing-to-Opening Pressure Ratio

Both events are thresholds on the same falling upstream pressure: the valve opens when it reaches Δp_{open} above the downstream pressure, and flashing begins when it reaches the saturation pressure of the upstream fluid. Their order therefore follows from comparing $p_{sat}(T_0)$ with Δp_{open}, which the ratio $r = p_{sat}(T_0)/\Delta p_{open}$ expresses directly, the downstream pressure being small here. The ratio contains no information beyond the two threshold pressures themselves.

The r column of Table I orders the cases of both configurations. Cases with r below unity open within about ten seconds and those above unity are delayed by two to three orders of magnitude, although the configurations differ by more than a factor of three in initial pressure and by about 45 % in Δp_{open}. The calculated cases bracket the boundary only to $0.75 < r < 1.28$, opening at 9.9 s and 987 s respectively, and cases near unity have not been run. Within the delayed branch the opening time is not monotonic in r: the saturated inlet of configuration B has r = 10.0 and opens at 1625 s, earlier than the 300 °C case at r = 5.73. Once flashing precedes opening, the delay is set by how long the vessel takes to boil off rather than by the ordering of the two events. All saturated cases of one configuration also share a single r, so quality is a variable the ratio cannot see. A dry saturated vapour inlet cannot flash, so the criterion does not apply to it.

5.3 Disk Lift Oscillation

In the 185 °C case the disk rose to about 3.5 mm against a full-open position of about 11 mm and oscillated about that level, so first lift and full flow area are different events there. The damping is the lower bound of Section 2.1, taken from the practice of the relief-valve literature rather than chosen to produce this behaviour. Whether the motion is physical, a consequence of that bound, or an artefact of the coupled integration is not settled; the solution-verification items of Table II are what would separate the third from the first two.

5.4 Sensitivity to the Closure Model

The branch a case falls on and the length of its delay depend on the closure to very different degrees. Assigning a case to a branch is a comparison of the upstream saturation pressure with the opening differential pressure, and the closure computes neither, so the ordering is insensitive to it. The magnitude of the delay is a different matter, because it is set by how fast the vessel empties once it is two-phase, which is exactly what the closure computes. The delayed times in Table I therefore give the order of magnitude of the stall rather than a predicted opening time.

6. Conclusions

A lumped multi-control-volume two-phase chamber model was coupled to the disk equation of motion and applied to the depressurization of the upstream vessel over a range of upstream fluid states. The following are concluded:

1) The upstream fluid state changes the calculated time of first lift by two to three orders of magnitude in both configurations. What separates the branches is whether flashing begins before or after the disk starts to lift, not when it begins.

2) Since both events are thresholds on the same falling pressure, that ordering is expressed by the ratio of the upstream saturation pressure to the opening differential pressure. The calculated cases are consistent with a boundary at unity but bracket it only to $0.75 < r < 1.28$, and the ratio does not order the delay within the delayed branch.

3) The verification completed so far covers the analytic anchors of the closure and the zero-flow check. The solution-verification items and the cross-comparison against independent closures are in progress, and validation has not been performed, so the results are presented as an interim status.

The subcooled branch of the closure has not been confirmed; the magnitude of the flow reduction depends on it, although the ordering of the two events does not. A valve-specific two-phase discharge coefficient has not been determined, and a single constant value cannot represent its variation with the flow regime. The steady flow force is omitted and each vessel is a single homogeneous node, which is likely to matter most for the delayed cases in which a real vessel would stratify. The single-phase comparison, the cases near the branch boundary and the separation of the Section 5.3 oscillation from a numerical artefact are the subject of the continuing work, on which comments would be welcome.

ACKNOWLEDGEMENT

This work was supported by the Innovative Small Modular Reactor Development Agency grant funded by the Korea Government (Ministry of Science and ICT, MSIT) (No. RS-2023-00321928).

REFERENCES

[1] Young-seok Bang, Young-jae Park, You Cho Choi, Seong-Su Jeon, Soon-Joon Hong, Application of MATLAB to Predict Dynamic Behavior of PECCS Valves of i-SMR, Transactions of the Korean Nuclear Society Autumn Meeting, Changwon, Korea, October 30-31, 2025.

[2] Jeong-won Han, Young-seok Bang, Young-jae Park, Preliminary Study on a Simplified Two-Phase-Flow Model for the Dynamic Response of Passive Emergency Core Cooling System Valves, [TBD proceedings], 2026.

[3] Mohammad Rezay Burhani, Csaba Hos, Estimating the opening time of a direct spring operated pressure relief valve in the case of multiphase flow of fixed mass fraction in the absence of piping, Journal of Loss Prevention in the Process Industries, 66, 104169 (2020).

[4] Joseph C. Leung, A generalized correlation for one-component homogeneous equilibrium flashing choked flow, AIChE Journal, 32, 1743-1746 (1986).

[5] Giovanni Boccardi, Roberto Bubbico, Gian Piero Celata, Barbara Mazzarotta, Two-phase flow through pressure safety valves. Experimental investigation and model prediction, Chemical Engineering Science, 60, 5284-5293 (2005).